ZACube-2 Mission Operations Analysis

Gregory J. Naidoo, Robert van Zyl, and Gunjan Gupta

Abstract This research entails a comprehensive analysis of ZACube-2 operational mission data which addresses on-orbit operations. The mission operations evaluation criteria that will be investigated include all available telemetry, tracking, and command datasets at system and subsystem levels, with the orbital dynamics of the system and the ground segment operations. An auxiliary analysis will investigate space weather and its effects on the mission about how the system reacts in the presence of solar activity over particular areas of the Earth, which will provide an assessment of overall system robustness. The research output will give an objective evaluation of the operational performance of the system comprising space and ground segments against the mission design specifications. It will compare the as-designed features of the satellite with actual system performance. Design improvements will be recommended for incorporation in the design cycle of future missions.

Keywords Telemetry · ZACube-2 · Mission operations · System performance · Mission analysis · Orbital dynamics

1 Introduction

Long-range radio (LoRa) is mainly used for machine-to-machine (M2M) and the Internet of Technology (IoT); however, they are gaining attention for satellite communication [1–3]. In [4], a survey of satellites launched, and timelines have been conducted. In [5–7], the launch of satellites with different payloads and controller types is compared. The ZACube-2 mission is the second satellite developed in the Cape Peninsula University of Technology (CPUT) Satellite Programme, hosted by French South African Institute of Technology (F'SATI) with funding from the Department of Science and Innovation. The satellite is a 3-unit (3U) CubeSat and

G. J. Naidoo (✉) · R. van Zyl · G. Gupta
French South African Institute of Technology, Department of Electrical, Electronics and Computer Engineering, Cape Peninsula University of Technology, Cape Town, South Africa
e-mail: naidoogr@cput.ac.za

A. Kumar et al. (eds.), *Proceedings of the 4th International Conference on Data Science, Machine Learning and Applications*, Lecture Notes in Electrical Engineering 1038,
https://doi.org/10.1007/978-981-99-2058-7_24

was launched in 2018 with the prime objective of providing sovereign maritime-domain awareness services in support of Operation Phakisa, an initiative supporting the National Development Plan (Operation Phakisa). A novel fire detection imager was also demonstrated as a secondary mission objective.

The technology and mission roadmap of the CPUT Satellite Programme aims to continually support national imperatives, such as the National Development Plan. The immediate development is toward a constellation of satellites that deems to complement and further develop the maritime communications services, as demonstrated by ZACube-2. The mission, therefore, is of critical strategic importance to the South African space industry as it serves as the baseline design for future missions and programs.

To this end, evaluating the satellite's operations against its primary mission objectives and to validate and improving the design approach that will be incorporated in future missions is imperative. By doing so, more effective and reliable methods across the full-design lifecycle of the mission can be adopted, contributing to the longevity of the South African space industry.

2 Methodology for Resource Budgets Analysis

The purpose of this analysis is to validate the various budgets that were used to design ZACube-2 operations. These budgets include power, thermal, mass, and link budgets, and the mass budget does not require verification through telemetry analysis.

Validation of the various budgets is essential as it guides the development of the next iteration of CubeSats, relaying information on areas of improvement. A prime example would be comparing different power profile versions, with one being calculated or simulated and the other being calculated directly from the telemetry.

2.1 Power Budget

ZACube-2 has four power profiles describing the calculated power used when that profile is activated, either when the CubeSat is in a minimal solar condition or experiencing the maximum eclipse (Table 1).

To calculate the telemetry-based values for the various profiles, a random day when the profile activation criterion was met was chosen, and the average power was calculated in the period in which the respective profile was active (Table 2).

The subsystems that are vital in the basic operation of ZACube-2 require power to operate

- UHF transceiver.
- Electronic power supply.
- Battery.

Table 1 ZACUBE-2 power profiles description

Power profile	Description
Safe sun/eclipse	Basic safe mode with most of the bus in idle and payload off
Safe TTNC sun/ eclipse	Safe mode with TTNC session and most of the bus in idle and payload off
Downlink sun/ eclipse	Downlink mode with TTNC session, data downlink, and most of the bus in idle and payload off
Payload sun/ eclipse	Payload operations with TTNC session, data downlink, and most of the bus in idle and payload on for one pass

Table 2 ZACUBE-2 power profile condition

Power profile	Non-vital subsystem active
Safe sun	Only the vital subsystem
Safe TTNC sun	S-band transmitter
Downlink sun	S-band transmitter, UHF transceiver
Payload sun	Software-defined radio, K-line imager, S-band transmitter

- On-board computer.
- Attitude determination control system.

In addition to validating the power profiles, analysis of both the battery and the solar array is necessary as these two subsystems are essential in ensuring power to the spacecraft.

For the battery voltage, close inspection will be taken to the depth of discharge, which is in the power budget and, following the manufacturer's recommendations, was described at a maximum of 20%, which for an 8.4 V capacity battery is 6.72 V shown in Fig. 1.

Various "profiles" were described for the solar array; however, these profiles were configurations with each configuration being a scenario on what panels were illuminated and how much power was being produced. The minimum power generated was described as 6.4717 Wh shown in Fig. 2. To calculate this, the same method that was used to calculate the power profiles is used.

2.2 Thermal Budget

The thermal budget is used to simulate the thermal working conditions at which the satellite will operate and verify if there is enough thermal headroom for the various subsystems to operate effectively and efficiently.

To simulate this environment, two methods were employed, namely [8, 9], respectively, with the latter being the most commonly used in industry. While these two

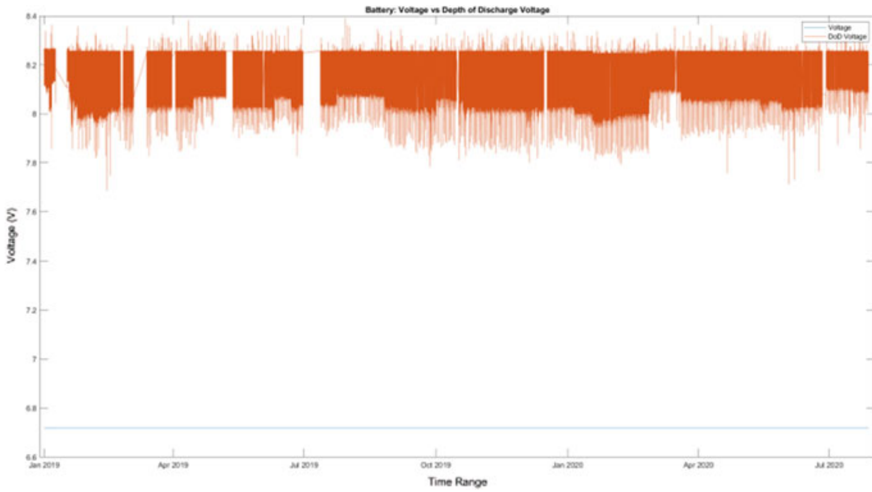

Fig. 1 Battery voltage versus depth of discharge voltage

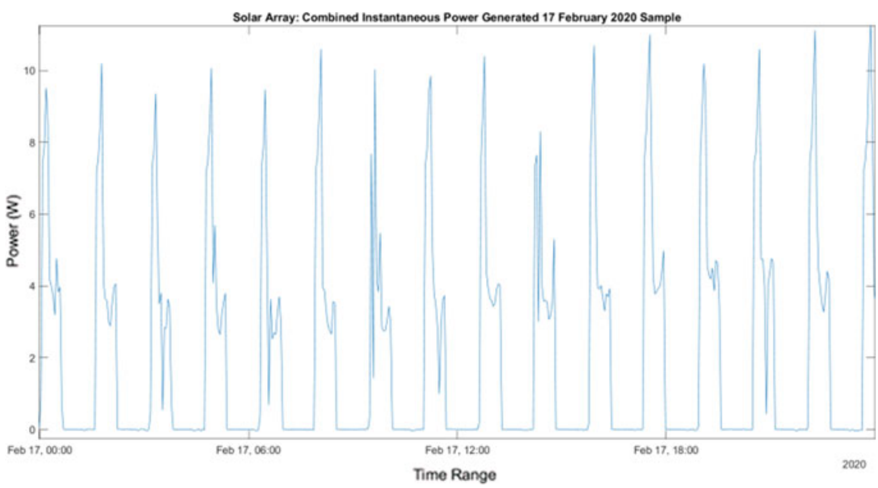

Fig. 2 Solar array combined instantaneous power generated February 17, 2020, sample

methods are similar, the methodology described in [8] is more comprehensive as it is based on actual telemetry instead of being altitude and inclination dependent.

In the aforementioned method, both yield an approximate thermal balance when the satellite is sunlit and in eclipse conditions which makes the satellite experiencing maximum and minimal heat dissipation. Once the maximum and minimum temperatures were calculated, it was compared with individual thermal telemetry channels to check whether the telemetry exceeded the calculated temperatures and the manufacturer's thermal limits [10–14].

2.3 *Link Budget*

A link budget is a set of calculations to consider whether the satellite makes a good link with the ground station at various elevation angles, ensuring no packet loss. An accurate means of measuring the link integrity is to analyze the RSSI or received signal strength indicator telemetry [15].

The ground station could communicate is already known as data was being sent and received, and the only things need to be learned are the performance of the link. To verify this, the RSSI telemetry, which is given in voltage, was cross-referenced with Table 3 that showed the RSSI value signal strength equivalent [16].

2.3.1 Resource Budgets Results

After completing the power, thermal, and link budget, the telemetry-based results were compared with the designed resource budgets.

2.3.2 Power Budget

In Table 4, various power profiles are compared. It should be noted that there is telemetry data for the eclipse profile due to no operation.

Table 3 UHF RSSI voltage value to signal strength

RF level (dBm)	Voltage (V)		
	Minimum	Typical	Maximum
− 118	N/A	0.3	0.8
− 68	0.7	1.1	1.8
− 23	1.2	1.8	2.5

Table 4 Comparison of power profiles

Profile name	Power consumed (Wh)		
	Power budget	Telemetry	Difference
Safe sun	1.759	1.705	0.054
Safe eclipse	1.068	1.049	0.019
Safe TTNC sun	2.576	2.101	0.354
Safe TTNC eclipse	1.885	1.583	0.274
Downlink sun	3.576	2.848	0.728
Downlink eclipse	1.432	1.408	0.024
Payload sun	4.976	2.297	2.679
Payload eclipse	4.285	N/A	N/A

Table 5 Solar array configuration calculation results

Profile name	Power (Wh)
Calculated value from sample	3.3869
Sun on 3U	6.4717
Difference	− 3.0848

Table 6 Comparison of thermal telemetry limits for various subsystems

Parameter	Temperature (°C)		
	Maximum	Minimum	Range
Battery	31.9865	− 8.4731	40.4596
K-line imager	29.1500	− 15.1250	44.2750
S-band transmitter	37.2314	13.8672	23.3642
UHF transceiver	28.0000	− 11.0000	35.0000
Fortescue	49.2125	− 21.4518	80.6643
Gilmore	43.3290	− 21.0940	64.4230

The battery voltage, which has taken over the span of the available telemetry, was compared to the calculated maximum depth of discharge (DoD) described in the power budget, which is 6.72 V.

The solar panel average power is generated on a random day to see if enough power is available to operate both the spacecraft and charge the battery for operation when in eclipse.

Using the figure above, a value can be calculated of the average generated power when the satellites are in view of the sun. This telemetry value can then be compared to the calculated stipulated in the power budget. This can be seen in Table 5.

2.3.3 Thermal Budget

In Table 6, the maximum and maximum telemetry temperatures for the various subsystems are compared. This is done to show the thermal range that each respective subsystems experiences over temporal span that the telemetry was taken from.

2.3.4 Link Budget

A combination of a Gaussian probability function and a cumulative density function (CDF) was generated to verify the integrity of the link [17].

3 Discussion of Results

With the results being generated from the aforementioned data analysis, comments on the performance can be made on whether the telemetry metrics fit within the system's expectations derived from the resource budgets.

3.1 Power Budget

From Table 4, it can be seen that overall, the power budget values are higher than the ones calculated using the respective telemetry and within a 1 Wh margin. The most significant difference between the telemetry-derived values and the power budget can be seen when the payload sun is active, where only 46.1616% of the power specified in the power budget was used [18].

The reason behind the significantly lower power value was that during the calculation, the different subsystems had different data logging times, leading to the recording of power values in one subsystem, while the other subsystem is not logging data. While linear interpolation can be used to replace missing values, it is not an accurate representation of the data recorded; additionally, this brings up an issue that not all the subsystems data are logged at the same time interval [19, 20].

The battery used for ZACube-2 has a charge limit of 8.4 V; therefore, this equates to a minimum battery charge of 6.72 V or a discharge value of 1.98 V. However, the maximum and minimum values were found to be 8.3917 V and 7.6849 V, respectively, indicating that the maximum discharge voltage experienced was 0.7068 V which is far smaller than the specified discharge value of 1.98 V.

Maximum discharge, when calculated as a percentage of the maximum charge limit of 8.4 V, gives a value below 8.42%, and likewise, the minimum discharge was calculated as 8.51%. Both of these telemetry values are less than that of the maximum designed depth of discharge value of 20%.

The solar array calculation showed the instantaneous peak power generated is approximately between 8 and 8.5 W; however, according to the telemetry calculations, only about 52.3340% of the required power was generated when comparing to the value required in the power budget. The exact process was replicated using a different time period to perceive if the first instance was an anomaly. The results from these two sample calculations are seen in Table 7.

Table 7 Difference in solar array telemetry configuration

Sample number	Date of telemetry sample (UTC)	Power (Wh)
1	February 17, 2020	3.3869
2	March 15, 2019	4.4171
	Difference	1.0302

From Table 7, the second sample calculation is 130.4171% larger than the total power generated from sample 1 which as clarified before is only 52.3340% of the minimum required power with sample 2 value only being 68.2525% of the aforementioned minimum required power stated in the power budget. Two pieces of information can be extracted from the sample calculations and could explain as to why these values differ and/or not being close to the required power value.

The first piece of information is that from the two sample calculations, the power being generated by the solar array does not meet the minimum required power in the power budget. However, the battery's voltage depth of discharge should be greater than the value specified in the power budget, i.e., 20% if the solar array failed to meet this minimum required value. Yet, the calculated depth of discharge was found to be 8.42%, well within the 20% margin. In this case, telemetry data was logged at an interval of 3 min.

The second piece of information is that sample values variate at 1.0302 Wh. This variance can be accredited to the combination of two factors: solar declination and/or whether the sun is in solar minimum or maximum. Due to the Earth's rotational axis being off-center as the Earth rotates around the sun, the declination angle variates over the year. This affects the angle at which the solar rays hit the solar panels and in turn the power produced [21].

The second factor is whether the sun is in solar minimum or maximum also referred to as the solar cycle. The solar cycle is experienced by the sun where approximately every 11 years, the density of sunspots increases or decreases, respectively, where the number of sunspots directly affects the strength of the UV radiation and as such the power generated. In the telemetry range that was used to calculate the sample values, it was found that the sun experienced solar minimum, and subsequently, there was minimal number of sunspots, therefore less power being generated [22].

From Table 5, the power budget values are higher than the ones calculated using the respective telemetry and within a 1 Wh margin. The largest difference between the telemetry-derived values and the power budget can be seen when the payload sun is active, where only 46.1616% of the power specified in the power budget was used. While linear interpolation can be used to replace missing values, it is not an accurate representation of the data recorded; additionally, not linearly interpolating brings up an issue that not all subsystem data is logged at the same time interval [23].

3.2 Thermal Budget

From Table 6, which shows the available thermal telemetry and said range of the various respective subsystems, i.e., battery, K-line imager, S-band transmitter, and the UHF transceiver. What can be seen is that the S-band transmitter experiences the highest temperature of 37.2314 °C with the lowest temperature being experienced by the K-line imager of 15.1250 °C. These values co-inline with the operational behavior of the satellite as the S-band transmitter provides a high-speed downlink, which requires more power to the ground station, therefore incurring a higher thermal value.

While the K-line imager being the hosted payload is not used as frequently in comparison with the communications-based subsystem, therefore having a lower thermal value. While temperature can be somewhat be seen as a measure of how frequent and/or how much power said subsystem consumes, this is only an implied notion as multiple factors such as thermal control and operational scheduling play a vital role in which affects the subsystem temperature.

The results in Table 6, in particular the last two rows, additionally show that the method that employs calculation techniques from [9] has a larger thermal range when compared to the method that employs calculation techniques from [8], suggesting that both are valid approaches. The method described by Fortescue et al. [9] is more conservative than that described by Rashid et al. [8], e.g., the latter method produces results that are more in line with actual performance, and as such, there is not much thermal headroom [10].

Telemetry from the battery, UHF transceiver, and S-band transmitter showed that the respective subsystems thermally performed within the manufacturer's specifications with additional headroom. What this means practically is that the passive thermal control techniques employed on ZACube-2 worked as designed.

Using Tables 8, 9, and 10, the averaged thermal performance of the respective subsystem is well within the limits specified by the manufacturer, especially in the case when looking at the values described in Table 9, with there being more thermal headroom when the respective subsystems are experiencing maximum temperature in comparison with the minimum temperature thermal headroom.

Two approaches were taken to manually calculate the thermal range that would be experienced by ZACube-2, while it is vital to compare these approaches to one another, and a comparison between the two approaches and the thermal telemetry is needed as well.

From Table 11 in relation to the thermal telemetry from ZACube-2, the hand calculation that employs [8] method is more in line with the thermal telemetry

Table 8 Comparison of battery thermal telemetry and manufacturer specifications

Parameter	Temperature (°C)		
	Telemetry	Manufacturer	Difference
Maximum	31.9865	50	18.0135
Minimum	− 8.4731	− 10	1.5269

Table 9 Comparison of UHF transceiver thermal telemetry and manufacturer specifications

Parameter	Temperature (°C)		
	Telemetry	Manufacturer	Difference
Maximum	28	61	33
Minimum	− 11	− 25	14

Table 10 Comparison of S-band transmitter thermal telemetry and manufacturer specifications

Parameter	Temperature (°C)		
	Telemetry	Manufacturer	Difference
Maximum	37.2314	61	23.7686
Minimum	13.8672	− 25	11.1328

Table 11 Comparison of thermal hand calculation techniques in relation to temperature telemetry

	Thermal hand calculation temperatures (°C)			
	Fortescue		Gilmore	
	Minimum	Maximum	Minimum	Maximum
Thermal telemetry (°C)	− 21.4518	49.2125	− 21.0940	43.3290
Minimum	− 15.1250		− 15.1250	
Maximum		37.2314		37.2314
Difference	6.3268	11.9811	5.9690	6.0976

compared to the method described by Fortescue et al. [9] in addition to having a smaller thermal headroom when comparing maximum temperatures in relation to the telemetry temperatures.

3.3 Link Budget

When cross-referencing the values in Table 3 in relation to Figs. 3 and 4, it can be seen that the lowest RSSI value is 1V which means that anything below that value would be considered noise because the transceiver does not have the functionality to process signals weaker than – 116 dBm. Therefore, by looking at the *x*-axis of the UHF transceiver, RSSI cumulative probability function graph the percentage of the received signal which is noise can be determined.

By looking at the graph at 1 V, this correlates to a cumulative value of 89.1896%, what this means is that less than 89.1896% of signals processed by the transceiver is noise with only 10.8104% of the signals be interpreted or useful. This value can be seen as how well the transceiver works seeing as the ground segment did indeed receive the data from ZACube-2.

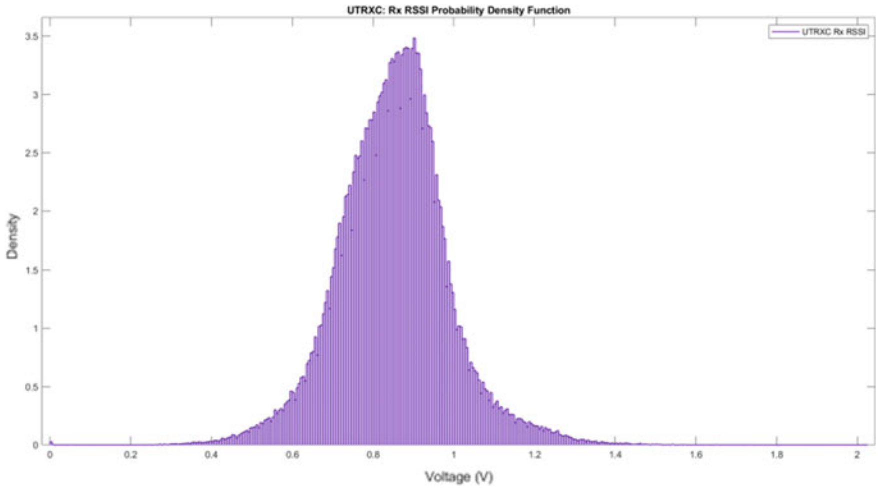

Fig. 3 UHF transceiver RSSI probability density function

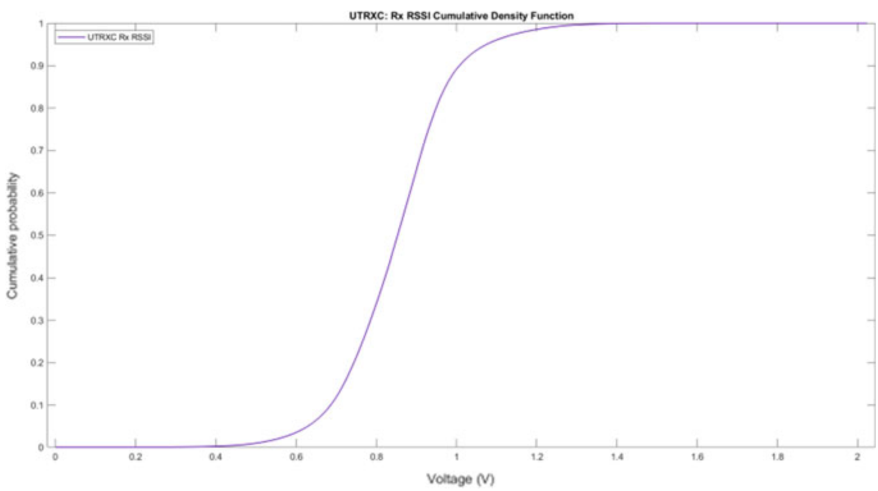

Fig. 4 UHF transceiver RSSI cumulative density function

4 Conclusion

Using the output of this assessment, design improvements can be recommended for incorporation in the design cycle of future missions. Therefore, not only improving the satellite regarding how effective and efficient mission operations are executed but also further improving upon the satellite design expertise of the engineering team.

From the discussions that were had in the previous sections regarding the performance at a systems-level, e.g., the various resource budget as well as at a subsystems level. Additionally, problems that arose will be a discussion from an objective view.

4.1 Power Budget

ZACube-2 had six power profiles and two power-related profiles which were the orbital periods and minimum power generated by the solar array. All six of the power profile values, apart from the payload eclipse as the imager was not operated in eclipse, were lower than the values calculated in the power budget suggesting that the power budget was conservative.

As for the conservative metric, on the lowest end of the spectrum, the safe eclipse telemetry-based value was only 1.7790% smaller, while on the highest end of the spectrum, the payload sun telemetry-based value was 53.8384% smaller than the power budget value. The reason why there was such a drastic difference in power level is that there was no common interval at which the telemetry data was logged causing missing respective values across the respective subsystems. This dissimilarity was accredited to the variating solar declination that is experienced throughout the year as the sample was calculated on March 15, 2019, UTC and February 17, 2020, UTC, respectively.

Furthermore, the difference could be a trait of the solar cycle progression as the range of telemetry value that was used in calculation occurred when at solar minimum, e.g., transition phase between solar cycle 24 and solar cycle 25.

With both telemetry sample calculations conveying that not enough power was being generated to sustain the needs of the satellite, there should be large amounts of discharge from the battery to provide that remaining power needed. However, battery discharge was minimal at 8.42% conveying that either method in which the power values were calculated is incorrect or the problem lies within the telemetry values.

4.2 Thermal Budget

From the telemetry, the largest thermal range experienced by a single subsystem was the K-line imager of 44.2750 °C with a maximum of 29.15 °C and a minimum of −15.1250 °C.

The S-band transmitter had the maximum overall temperature from any subsystem of 37.2314 °C with the K-line imager having the lowest temperature logged from any subsystem. All the subsystems performed well within the thermal limits specified by the manufacturer implying that passive thermal management techniques employed on ZACube-2 worked as desired leaving thermal headroom for either switching subsystems on longer, if there is power available, or if the stacking order of the subsystems needs to be changed.

Telemetry-based thermal values were compared to the two methods, the first method described by Maharaj et al. [2] and the second method described by Gupta and Van Zyl [1].

The first method had the largest thermal range of 80.6643 °C with the second method having a thermal range of 64.4230 °C this directly translated to the [1] variance in maximum and minimum values being within 6.0976 °C and 5.9690 °C, respectively, whereas [2] maximum and minimum values were 11.9811 °C and 6.3268 °C respectfully.

From this, it can be seen that to give a rough idea of the thermal range as well as the expected maximum and minimum temperatures, the satellite should experience before a computer simulation, and the method described by Gupta and Van Zyl [1] should be used.

4.3 Link Budget

Knowing that the UHF transceiver does make successful contact with the ground station as there is communication, it was a matter of verifying how well the UHF transceiver link works.

Using cumulative probability function, the Rx RSSI of ZACube-2 UHF transceiver was plotted, in conjunction using the signal strength to voltage table provided in the UHF transceiver hardware report, and it was found that 89.1896% of the RSSI signal was noise.

5 Recommendations for Future Work

While objectively it can be said that ZACube-2 works as the system did produce enough power to still be operational, communicated with the ground station, and never experienced any difficulties that are associated with poor thermal management, there were points of interest that could be implemented which would make it easier for future telemetry analysis on the next iteration of satellites.

- Recalculation of solar array results as the information relayed by the telemetry does not accurately depict the actual performance.
- Examination of a broader spectrum of space weather events that possibly caused the same events of no telemetry or outlier data to be present in multiple telemetry channels.
- Possibility of synchronizing the interval at which telemetry across multiple channels is logged.
- Pre-set exposure threshold to account for antenna reflections or consider either relocating the ADCS to mitigate issues related to reflection from the sun.

- Complete a computer simulation of ZACube-2 thermal performance to confirm that all thermal parameters are met and to confirm that the method described by Gupta and Van Zyl [1] is a good basis prior simulation.
- Have individuals who have more experience in the respective field to view the data and draw conclusions separately.

References

1. Gupta G, Van Zyl R (2022) NOMA-based LPWA networks. In: Expert clouds and applications. Lecture notes in networks and systems, vol 209. pp 523–530. https://doi.org/10.1007/978-981-16-2126-0_42
2. Maharaj R, Balyan V, Khan MTE (2022) Optimising data visualisation in the process control and IIoT environments. Int J Smart Sens Intell Syst 15(1):1–14
3. Maharaj R, Balyan V, Khan MTE (2022) Design of IIoT device to parse data directly to scada systems using LoRa physical layer. Int J Smart Sens Intell Syst 15(1):1–13
4. Gupta G, Van Zyl R (2022) Survey based on configuration of CubeSats used for communication technology. Adv Intell Syst Comput 1235:59–71. https://doi.org/10.1007/978-981-16-4641-6_6
5. Prasad PS, Sunitha Devi B, Janga Reddy M, Gunjan VK (2019) A survey of fingerprint recognition systems and their applications. Lecture notes electrical engineering, vol 500. pp 513–520
6. Jan YW, Chiou JC (2005) Attitude control systemfor ROCSAT-3 microsatellite: a conceptual design. Acta Astronaut 56(4):439–452
7. Rudra Kumar M, Pathak R, Gunjan VK (2022) Diagnosis and medicine prediction for COVID-19 using machine learning approach. In: Computational intelligence in machine learning: select proceedings of ICCIML 2021. Springer Nature Singapore, Singapore, pp 123–133
8. Rashid E, Ansari MD, Gunjan VK, Ahmed M (2020) Improvement in extended object tracking with the vision-based algorithm. In: Modern approaches in machine learning and cognitive science: a walkthrough: latest trends in AI. pp 237–245
9. Fortescue P, Swinerd G, Stark J (2011) Spacecraft systems engineering, 4th edn. Wiley, Chichester
10. Wertz J, Larson W (1999) Space mission analysis and design, 3rd edn. Microcosm, Torrance, California
11. Lakshmanna K, Shaik F, Gunjan VK, Singh N, Kumar G, Shafi RM (2022) Perimeter degree technique for the reduction of routing congestion during placement in physical design of VLSI circuits. Complexity 2022:1–11
12. Kaminskiy M, Kashem N (2015) CubeSat data analysis revision—revision 2015. National Aeronautics and Space Administration, Maryland
13. Gaddam DKR, Ansari MD, Vuppala S, Gunjan VK, Sati MM (2022) A performance comparison of optimization algorithms on a generated dataset. In: ICDSMLA 2020: proceedings of the 2nd international conference on data science, machine learning and applications. Springer Singapore, pp 1407–1415
14. Kaminskiy M (2015) Cubesat data analysis revision. National Aeronautics and Space Administration, Greenbelt, Maryland
15. Kolhe NP, Dhote KK, Parihar A (2023) Mapping the access of internet facility to schedule tribe population—an approach towards digital education. In: Digital learning based education: transcending physical barriers. Springer Nature Singapore, Singapore, pp 1–20
16. Muthmainnah, Ganguli S, Al Yakin A, Ghofur A (2023) An effective investigation on YIPe-learning based for twenty-first century class. In: Choudhury A, Biswas A, Chakraborti S

(eds) Digital learning based education. Advanced technologies and societal change. Springer, Singapore. https://doi.org/10.1007/978-981-19-8967-4_2
17. Ganguli S, Al Yakin A (2023) An effective investigation on YIPe-learning based for twenty-first century class. In: Digital learning based education: transcending physical barriers. Springer Nature Singapore, Singapore, pp 21–38
18. Pathak R, Gupta SS (2020) A study on natural computing: a review. In: ICDSMLA 2019: proceedings of the 1st international conference on data science, machine learning and applications. Springer Singapore, Singapore, pp 1975–1983
19. Chatterjee R, Bandyopadhyay A, Chakraborty S, Dutta S (2023) Digital education: the basics with slant to digital pedagogy-an overview. In: Digital learning based education: transcending physical barriers. pp 63–80
20. Das N (2023) Digital education as an integral part of a smart and intelligent city: a short review. In: Digital learning based education: transcending physical barriers. pp 81–96
21. Pathak R, Soni B, Muppalaneni NB (2023) Role of blockchain in health care: a comprehensive study. In: Gunjan VK, Zurada JM (eds) Proceedings of 3rd international conference on recent trends in machine learning, IoT, smart cities and applications. Lecture notes in networks and systems, vol 540. Springer, Singapore. https://doi.org/10.1007/978-981-19-6088-8_13
22. Nandy D, Majee D (2023) Socio-economic relations in digital education: a comparative study between Bangladesh and Nepal. In: Digital learning based education: transcending physical barriers. Springer Nature Singapore, Singapore, pp 103–117
23. Bhowmik T, Majumdar S, Choudhury A, Banerjee A, Roy B (2023) Importance of internal and external psychological factors in digital learning. In: Digital learning based education: transcending physical barriers. Springer Nature Singapore, Singapore, pp 119–132